CESEM

Center for Earth Systems Engineering and Management

Assessing Future Extreme Heat Events at Intra-urban Scales: A Comparative Study of Phoenix and Los Angeles

PROJECT WEBSITE
www.urbantransitions.org/extremeheat/

Matthew D. Bartos, Research Engineer
matthew.bartos@asu.edu

Mikhail V. Chester, Assistant Professor
mchester@asu.edu

SSEBE-CESEM-2014-WPS-001
Working Paper Series

12 June 2014

ASSESSING FUTURE EXTREME HEAT EVENTS AT INTRA-URBAN SCALES: A COMPARATIVE STUDY OF PHOENIX AND LOS ANGELES

Matthew D. Bartos
Research Engineer
matthew.bartos@asu.edu

Mikhail V. Chester, Ph.D.
Assistant Professor
mchester@asu.edu

Civil, Environmental, and Sustainable Engineering
Arizona State University
www.urbantransitions.org/extremeheat/

A research project "Prioritizing Cooling Infrastructure Investments for Vulnerable Southwest Populations" (www.urbantransitions.org/southwestheat/) between Arizona State University and the University of California Los Angeles. Supported by the National Science Foundation (Award Nos. 1335556 and 1335640).

Abstract

Already the leading cause of weather-related deaths in the United States, extreme heat events (EHEs) are expected to occur with greater frequency, duration and intensity over the next century. However, not all populations are affected equally. Risk factors for heat mortality—including age, race, income level, and infrastructure characteristics—often vary by geospatial location. While traditional epidemiological studies sometimes account for social risk factors, they rarely account for intra-urban variability in meteorological characteristics, or for the interaction between social and meteorological risks. This study aims to develop estimates of EHEs at an intra-urban scale for two major metropolitan areas in the Southwest: Maricopa County (Arizona) and Los Angeles County (California). EHEs are identified at a 1/8-degree (12 km) spatial resolution using an algorithm that detects prolonged periods of abnormally high temperatures. Downscaled temperature projections from three general circulation models (GCMs) are analyzed under three relative concentration pathway (RCP) scenarios. Over the next century, EHEs are found to increase by 340-1800% in Maricopa County, and by 150-840% in Los Angeles County. Frequency of future EHEs is primarily driven by greenhouse gas concentrations, with the greatest number of EHEs occurring under the RCP 8.5 scenario. Intra-urban variation in EHEs is also found to be significant. Within Maricopa County, "high risk" regions exhibit 4.5 times the number of EHE days compared to "low risk" regions; within Los Angeles County, this ratio is 15 to 1.

Table of Contents

1 Introduction 3
1.1 Definition of Extreme Heat Events 4
2 Methodology 5
2.1 Selection of Extreme Heat Event Criteria 5
2.1.1 National Weather Service "Excessive Heat" Criteria 6
2.1.2 Spatial Synoptic Classification System 7
2.1.3 Threshold Temperature Approach 8
2.2 Quantification of Extreme Heat Events 8
3 Results 9
3.1.1 Extreme Heat Events in Maricopa County 10
3.1.2 Extreme Heat Events in Los Angeles County 15
3.2 Conclusion 20
3.3 References 21
4 Appendix A 24
5 Appendix B 26

1 Introduction

Extreme heat events (EHEs) are the leading cause of weather-related deaths in the United States (NWS 2009). Between 2000 and 2009, excessive heat accounted for 24% of weather-related deaths in the U.S., with a total of 7,800 heat-related fatalities (CDC 2013). Heat waves often strike without warning, resulting in large numbers of fatalities over a short period of time. The 1995 Chicago heat wave resulted in the loss of over 700 lives over the course of a single week (Klinenberg 2002; Semenza et al. 1996. Whitman et al. 1997), while the European heat wave of 2003 resulted in 22,000-52,000 excess deaths across western and central Europe over a several-week period (Larson 2006). In addition to causing excess deaths, extreme heat can induce a number of heat-related illnesses (including rashes, cramps, heat exhaustion and heat stroke) and can aggravate cardiovascular, respiratory and other pre-existing conditions (CDC 2013, Semenza et al. 1999). During periods of prolonged heat, excess hospitalizations from these heat-related illnesses may overwhelm the local medical infrastructure. The effects of the Chicago heat wave in particular were exacerbated by inadequate ambulance service and insufficient hospital facilities (Duneier 2004). By one account, the medical infrastructure was so taxed that the city coroner had to "call in nine refrigerated trucks to store the bodies" (Klinenberg 2002). Extreme heat events are expected to increase as the atmospheric concentration of anthropogenic greenhouse gases increases (IPCC, 2007). Periods of abnormally high temperatures are anticipated to become more frequent, more intense, and longer-lasting over the twenty-first century. As the threshold of human tolerance to high temperatures is crossed more frequently and for longer periods of time, so too are the impacts of extreme heat on human health expected to increase (Kalkstein and Greene 1997).

Extreme heat events do not affect all populations equally. Risk factors associated with heat-related morbidity (such as age, race and living conditions) often vary by geospatial location. Lack of access to an air conditioner (or the inability to pay for the electricity for running it) is linked to the disproportionate risk of heat-related morbidity and mortality among low-income, urban elderly in the United States (Kovats and Hajat, 2008, Semenza et al., 1996). Residence in a high-crime area and lack of access to transportation are also associated with heat-related deaths and hospitalizations. Not having access to reliable transportation, whether a car or public transit, may restrict the capacity to move to cooler areas and government-sponsored cooling stations during extreme heat events (Semenza et al., 1996). Living in a neighborhood with heat-island effects (low tree cover and high percentage of dark-colored, impervious surfaces) increases vulnerability (Stone et al., 2010). There is a positive correlation between increasing community poverty and the presence of impervious surfaces and a negative response relationship between community poverty and tree cover (Heynen and Lindsey, 2003, Landry and Chakraborty, 2009). Similarly, there is a positive correlation between the proportion of people of color and the proportion of impervious surfaces, as well as between reduced tree cover (Pincetl, 2010b, Pincetl et al., 2012). Even meteorological characteristics like temperature can vary by spatial location: in one study, it was found that affluent neighborhoods were several degrees cooler in the summer of 2003 than low-income neighborhoods (Harlan et al.

2006, 2008; Jenerette et al. 2007). These differences in temperature can be explained by differences in land cover (i.e. vegetation) and by the proximity of water bodies—both of which are more common in affluent neighborhoods.

Although the risk factors for extreme heat vulnerability vary by geospatial location, current heat warning systems and epidemiological studies fail to capture these intra-urban dynamics. The majority of epidemiological studies treat the city as a single unit when analyzing excess mortality in the wake of heat waves (Braga et al. 2002; Curriero et al. 2002; Michelozzi et al. 2006; Smoyer et al. 2000). Similarly, current heat warning systems rely on data from centrally-located weather stations, and thus fail to incorporate intra-urban variation in temperatures (Sheridan and Kalkstein 2004; Smoyer-Tomic and Rainham 2001). Given that risk factors for extreme heat mortality vary by geospatial location, a robust assessment of urban heat vulnerability must account for local variation in meteorological characteristics. This study develops downscaled estimates of historical and projected extreme heat events for Maricopa County (as a proxy for the Phoenix Metro Area) and Los Angeles County (as a proxy for the Los Angeles Metro Area). Accounting for geospatial variation is especially important in cities like Los Angeles, where the proximity of the ocean causes temperature to vary by ten degrees or more from coastal to inland locations (Maurer 2002). This study accounts for geospatial variation by using gridded, observed meteorological data (1/8-degree resolution) along with downscaled general circulation model projections to characterize extreme heat events at a sub-city scale. Extreme heat events are identified for both historical (observed) and future (modeled) periods using an algorithm that detects prolonged periods of abnormally high temperatures within gridded temperature datasets. The frequency and duration of EHEs are then analyzed to determine locations that are most vulnerable to extreme heat under modeled future scenarios.

1.1 Definition of Extreme Heat Events

There is no universally agreed-upon definition of an extreme heat event. Methodologies for identifying EHEs vary depending on the purpose of the analysis and the data available. The simplest and most common approach is to define an EHE as being a period of abnormally hot weather for a given time and location (CDC 2013). The Environmental Protection Agency (EPA), for example, defines extreme heat events as "periods of summertime weather that are substantially hotter and/or more humid than typical for a given location at that time of year" (U.S. EPA 2006). In the same vein, a commonly-used method for determining extreme heat events involves detecting days for which the daily maximum temperature exceeds a specific threshold temperature for a given location. These threshold temperatures are often based on percentiles of the historical record. Several studies have related extreme heat events to the exceedence of two threshold temperatures corresponding to the 97.5th and 81st historical percentiles of summertime temperatures (Meehl & Tebaldi 2004, Clarke et al. 2010).

Other approaches identify extreme heat events based on a combination of meteorological characteristics that are associated with heat-related morbidity and mortality. The National Weather Service (NWS) identifies extreme heat events using a metric of human-perceived temperature called the "heat index". The heat index (a function of temperature, humidity, and physiological characteristics) accounts for the human body's temperature-regulating abilities. The human body normally cools itself through perspiration, which rejects heat by evaporating water at the surface of the skin. When humidity is high, the vapor pressure of the surrounding air limits the evaporation of water from the skin, thereby increasing the risk of overheating. Thus, NWS issues "Heat Advisories" and "Excessive Heat Warnings" based on the severity and duration of the heat index at a given location. Other methods for identifying EHEs account for the human health effects of an even larger suite of meteorological characteristics. The Spatial Synoptic Classification (SSC) system "identifies weather situations that increase the incidence of adverse health outcomes" based on "simultaneous interactions from a … suite of meteorological conditions". This method places weather patterns into discrete categories based on the interactions of several meteorological parameters, including temperature, humidity, cloud cover, and wind speed. Weather categories (known as "synoptic air masses") are then divided into "offensive" air masses that produce adverse health effects (e.g. Dry Tropical [DT] and Moist Tropical Plus [MT+]) and "non-offensive" air masses (e.g. Dry Moderate [DM] and Dry Polar [DP]) which have minimal human health effects. The SSC system has shown skill in predicting human health impacts, outperforming the heat index system in some cases (Greene 2011). However, under rigorous controls, and taking many locations into account, the performance of the SSC system is similar to many simpler metrics (Hajat et al. 2010).

2 Methodology

2.1 Selection of Extreme Heat Event Criteria

Because there is no universally-recognized definition of an extreme heat event, criteria for identifying EHEs must be carefully selected to meet the needs of the project. Each approach offers its own strengths and weaknesses. However, EHE identification methods are ultimately assessed based on their ability to satisfy the core objectives of the project. The primary goal of the project is to develop downscaled estimates of both historical and future EHEs for both Phoenix and Los Angeles. Thus, to achieve the objectives of this project, EHEs must be defined such that the following data requirements are satisfied:

1) Data used to identify EHEs must be available at a sub-city spatial resolution.
2) Data used to identify EHEs must be available for both historical (observed) and future (projected) time periods at the same spatial and temporal resolution.
3) Data used to identify EHEs must be available for both Phoenix and Los Angeles, and must be comparable between the two cities.

In addition to these core criteria, there are a number of supplementary "desired" criteria. Although these criteria are not essential to achieving the project objectives, they affect the robustness, validity and reproducibility of the results:

1) Modeled data used to identify future extreme heat events should be as accurate as possible.
2) Criteria used to identify extreme heat events must exhibit a strong correlation with human health impacts.
3) Methods used to identify extreme heat events should be transparent and reproducible for any arbitrary set of meteorological parameters. In other words, "subjective" methods of classification should be avoided if possible.

Three EHE definitions are considered in this study: the National Weather Service (NWS) "Excessive Heat Warning" criteria; the Spatial Synoptic Classification (SSC) system, and the threshold temperature approach. Each of these three approaches is assessed with respect to the project objectives. Ultimately, the threshold temperature approach is found to best satisfy the needs of the project. The NWS and SSC classifications, while useful for predicting human health impacts, are ultimately found to be difficult to reconcile with the needs of the project, due to limitations in data availability and the subjectivity of the methodology. The following sections explain the strengths and limitations of each approach.

2.1.1 National Weather Service "Excessive Heat" Criteria

The excessive heat warning classification used by the NWS is a widely recognized metric for predicting heat morbidity and mortality. However there are difficulties associated with parameterizing the NWS method such that EHEs can be isolated from an arbitrary set of meteorological forcings. First, there is no universal algorithm for determining an "excessive heat day" under the NWS system. Criteria for issuing excessive heat warnings vary by region and time of season. A heat index of 104º F may trigger a heat advisory in Los Angeles, where summer temperatures are generally mild, but may not trigger a heat advisory in Phoenix, where high temperatures are encountered frequently. Similarly, a heat index of 104º F may trigger a heat advisory in April (when extreme heat is unexpected), but not in June (when the human body is more acclimated to high temperatures). These calibrations to the standard heat warning criteria are not explicitly codified. Ultimately, the decision to issue an excessive heat warning is at the discretion of local authorities, and thus, there is an element of subjectivity to classifying extreme heat events under the NWS system. Second, the heat index classification requires data on relative humidity, which is typically not included in downscaled GCM output data. Relative humidity can be estimated using a hydrological model, like the Variable Infiltration Capacity (VIC) model (Liang et al. 1994).

However, hydrological model outputs are subject to error accumulation. The VIC model requires inputs of daily precipitation, maximum temperature, minimum temperature and wind speed. For future scenarios, these inputs must be obtained from downscaled, modeled GCM outputs. However, the accuracy of GCM outputs vary widely from parameter to parameter. In general, temperature is the most accurate output product from GCM models (with a reanalysis correlation coefficient between 0.95 and 0.99), while GCM outputs for other meteorological parameters are typically less accurate: for instance, correlation coefficients for precipitation typically range between 0.4 and 0.7 (Covey et al. 2003). Because the VIC model requires inputs that may not be reliable under future scenarios (namely, precipitation and wind speed), modeled relative humidity is subject to error accumulation. Although the NWS heat index system may have skill in predicting heat-related morbidity and mortality, determination of excessive heat events is ultimately hampered by the accuracy of the meteorological inputs, and by the subjective calibration factors used for different time periods and geospatial locations. For these reasons, the NWS criteria are not used in the analysis presented in this study.

2.1.2 Spatial Synoptic Classification System

The Spatial Synoptic Classification (SSC) system has demonstrated skill in predicting heat-related morbidity and mortality, and in some cases outperforms the NWS system (Greene 2011). However, its usefulness is diminished by its limited support for sub-city spatial resolutions, incompatibility with downscaled GCM outputs, and methodological subjectivity in determining weather types. First, the SSC system is not intended for use with gridded meteorological data, and thus offers limited support for sub-city spatial resolutions. Within the SSC system, parameters associated with each weather type (e.g. temperature, humidity, cloud cover) are identified at major meteorological gauging stations (typically located at airports). Parameter values needed to "trigger" each weather type are unique to each gauging location. Because each major city in the United States has only one meteorological gauging station supported by the SSC model, the SSC system does not support classification of weather types at a sub-city resolution. Second, the SSC system requires meteorological parameters for which downscaled projections are not readily available. In particular, "humidity" and "cloud cover" are not available at a sub-city resolution. These parameters could be estimated using a hydrological model (like VIC); however, as previously mentioned, these outputs are subject to error accumulation, and are difficult to validate. Finally, within the SSC system, selection of weather types is partially subjective: for each station, characteristic weather types are selected "manually" based on "climatological knowledge" (SSC 2013). In other words, there are no explicit algorithms for determining weather types based on local meteorological parameters. The SSC identification procedure is "commonly referred to as a hybrid classification mechanism" because it "involves both subjective and automated components" (Hondula & Davis, 2010). Given that the SSC system requires "manual" parameterization of weather types, it is difficult to generalize the classification process for an arbitrary set of gridded meteorological forcings. Finally, the SSC

system is less effective at predicting mortality for locations that exhibit little variation in weather types (Greene 2011). For Phoenix, the weather type is generally "Dry Tropical" (an "offensive air mass") for most of the summer (SSC 2013). Thus, for Phoenix, air mass classification by itself does little to predict heat-related mortality. For these reasons, the SSC system is not used to classify EHEs in this study.

2.1.3 Threshold Temperature Approach

Given the difficulties inherent in producing downscaled projections of EHEs under the SSC and NWS systems, it is resolved to identify EHEs based on temperature only. This method is selected for a number of reasons: (1) gridded daily temperature data is available at a sub-city resolution (1/8 degree) for both historical (observed) and future (projected) time periods; (2) GCM projections of daily temperature are more accurate than projections of other meteorological parameters like precipitation or wind speed; and (3) daily maximum temperature demonstrates reasonable skill in predicting heat-related illness and mortality. One study has shown that a simple temperature-mortality relationship performed better than either the SSC system or the NWS heat index system for several cities in a controlled test (Hajat et al. 2010). For Phoenix, temperature may be a better predictor of heat-related morbidity than "weather types" or multi-parameter indices. Chuang et al. (2013) have demonstrated that for the City of Phoenix, heat-related emergency calls are more strongly correlated with temperature than with heat index.

2.2 Quantification of Extreme Heat Events

Based on the methodology used by Meehl & Tebaldi (2004), extreme heat events are identified with respect to two near-surface threshold temperatures: (a) the 97.5th historical percentile of daily maximum temperature for summertime months (hereafter referred to as T1), and (b) the 81st historical percentile of daily maximum temperature for summertime months (hereafter referred to as T2). In this context, "summertime months" refers to the months of June, July and August. T1 and T2 are determined for each 1/8-degree grid cell in Phoenix and Los Angeles using gridded observed historical temperature data (Maurer et al. 2002). For each grid cell, T1 and T2 are taken as the 97.5th and 81st percentiles (respectively) of June-August daily maximum temperatures for the period 1960-1990. The algorithm used to identify T1 and T2 for each grid cell was written in Python, and can be found in Appendix A. Extreme heat events (EHEs) are then identified and isolated based on the following criteria (Meehl & Tebaldi 2004):

1) Maximum daily temperature must be above T1 for at least three consecutive days.
2) The average maximum daily temperature for the period must be greater than or equal to T2.
3) The maximum daily temperature must be above T2 for every day in the period.

These three criteria are incorporated into a separate Python algorithm that extracts extreme heat event days from gridded daily maximum temperature data (shown in Appendix B). For historical extreme heat days, observed daily maximum temperature data at a spatial resolution of 1/8-degree are used (Maurer et al. 2002). For future extreme heat events, downscaled daily maximum temperature projections are taken from the CMIP5 multi-model ensemble archive (Reclamation 2013). These projected datasets use the Bias Corrected Constructed Analogue downscaling method. Due to processing time constraints, not all of the models are included in the analysis. Rather, outputs from three representative models are selected: "MPI ESM LR", "CSIRO MK3", and "GFDL ESM2G". The MPI and CSIRO models are chosen because their reanalysis products demonstrate some of the highest correlation coefficients when compared to observed data (Covey et al. 2003). The GFDL model is chosen because it has been used extensively in climate change studies focusing on the United States (Brekke et al. 2009, CCCC 2009). Three representative concentration pathways (RCPs) are considered: RCP 2.6, RCP 4.5, and RCP 8.5. These RCPs represent future greenhouse gas trajectories (i.e. projection scenarios), with RCP 2.6 representing the lowest greenhouse gas concentration and RCP 8.5 representing the highest greenhouse gas concentration. The full specifications for each model run can be seen in Table 1 below:

Table 1. Specifications of Models, Ensembles and Projection Scenarios Used

General Circulation Model (GCM)	Ensemble	Representative Concentration Pathways Used
MPI ESM LR	3	2.6, 4.5, 8.5
CSIRO MK3 6-0	5	2.6, 4.5, 8.5
GFDL ESM2G	1	2.6, 4.5, 8.5

3 Results

Extreme heat events are found to increase markedly under all modeled scenarios for both Phoenix and Los Angeles. In Phoenix, annual EHEs increase by a minimum of 340% (under the RCP 2.6 scenario) and by a maximum of 1800% (under the RCP 8.5 scenario). For Los Angeles, the increase in EHEs is more moderate, with a minimum increase of 150%, and a maximum increase of 840%. For both cities, increases to EHEs are sensitive to the RCP scenario selected. Climate change also affects the spatial distribution of EHEs. In Phoenix, the overall spatial variability in EHE

frequency decreases as more parcels are affected by EHEs for longer periods of time. In Los Angeles, EHEs are redistributed from coastal regions to the inland regions, likely due to decreased sensitivity to coastal advection. In general, GCM models predict similar numbers of EHEs. Agreement between GCM models is assessed by determining the number of EHEs predicted by each model, and then determining the coefficient of variation in the number of EHEs predicted between models. Coefficients of variation between models range from a low of 0.10 (Maricopa County, RCP 2.6) to a high of 0.40 (Los Angeles County, RCP 4.5).

3.1.1 Extreme Heat Events in Maricopa County

For Maricopa County, EHEs increase by 340-1800% under future scenarios, with the greatest increases taking place under the RCP 8.5 scenario. In general, results are consistent between models. The coefficient of variation between models ranges between a low of 0.10 under the RCP 2.6 scenario to a high of 0.36 under the RCP 4.5 scenario (see Table 3). Figures 1 through 3 show the frequency of EHEs for Maricopa County under both historical and projected time periods. For these three figures, future EHEs are derived from the GCM-modeled temperatures. Figures 1 through 3 use temperature outputs from the "MPI ESM LR", "CSIRO MK3" and "GFDL ESM2G" models, respectively. The vertical dotted line signifies the transition point between observed and modeled data (occurring at the year 2010). EHEs are measured on the vertical axis, while time (in years) is measured on the horizontal axis. For each year, EHEs are measured in terms of parcel-days. In this context, a parcel-day refers to one extreme heat day in one 1/8-degree by 1/8 degree parcel. Thus, it is possible to have more than 365 parcel-days of EHEs in one year because there are 266 parcels in the Maricopa County region and 365 potential EHE days (making the theoretical maximum number of EHEs 97,090 parcel-days per year). By the 2080s, EHE counts of 25,000-30,000 parcel-days per year are encountered. This means that by the end of the twenty-first century, 25-30% of the entire year can be considered an "extreme heat event".

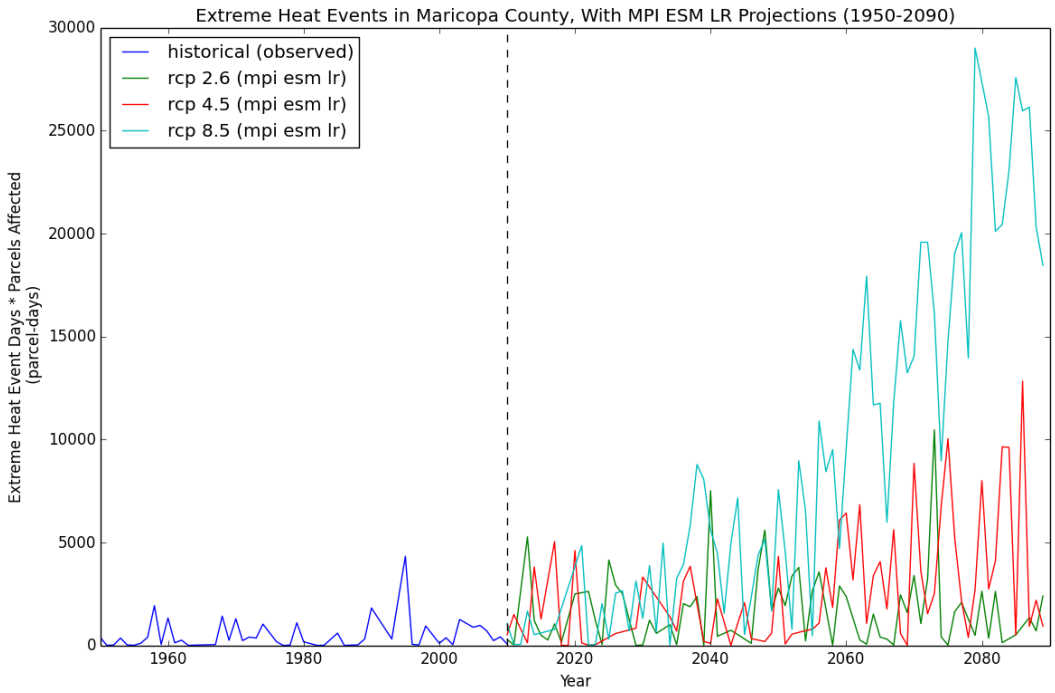

Figure 1. Extreme Heat Events in Maricopa County, with MPI ESM LR Projections (1950-2090).

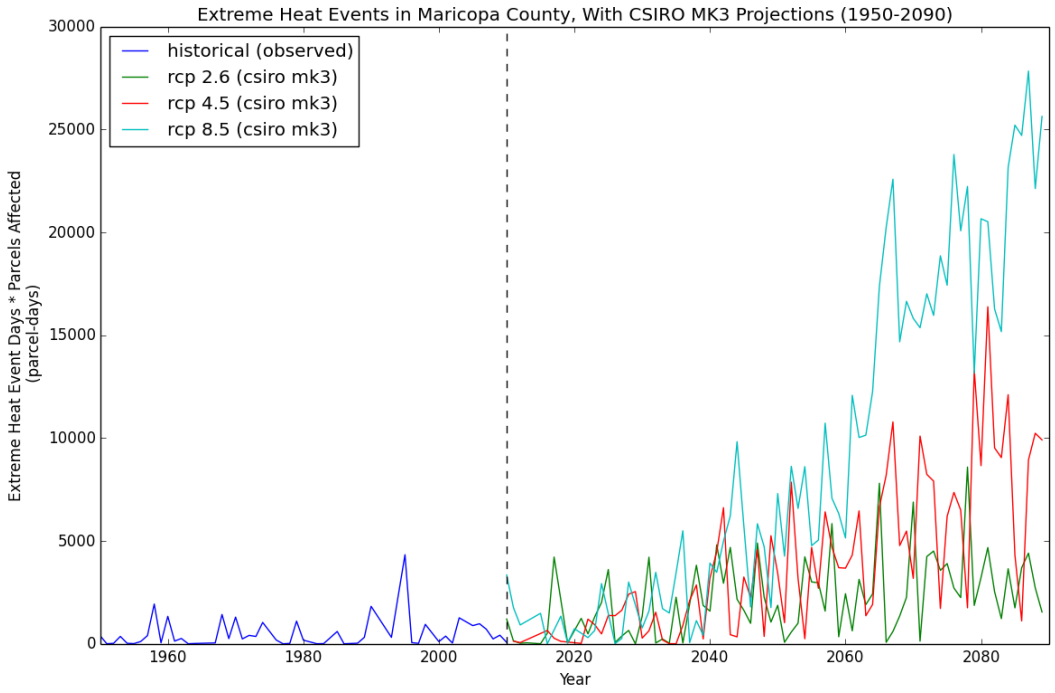

Figure 2. Extreme Heat Events in Maricopa County, with CSIRO MK3 Projections (1950-2090).

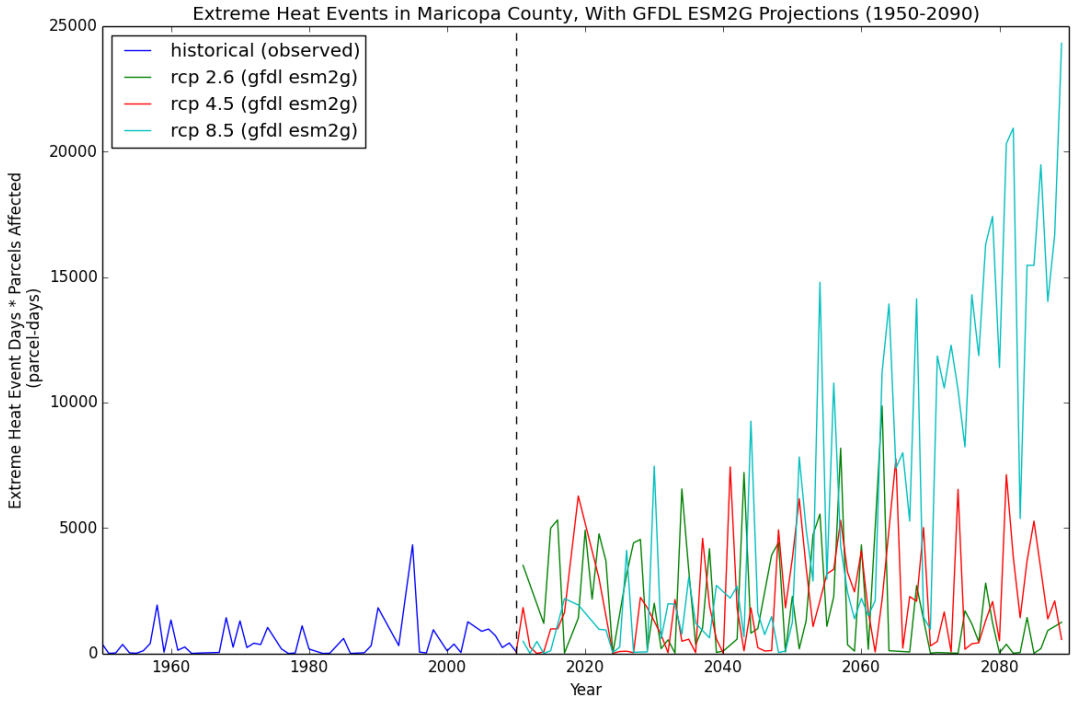

Figure 3. Extreme Heat Events in Maricopa County, with GFDL ESM2G Projections (1950-2090).

Table 2. Breakdown of Extreme Heat Events by Model and Scenario for Maricopa County.

Model/Scenario	RCP Scenario	Average Extreme Heat Events per Year (Parcel-Days)	Percent Increase in Extreme Heat Events
Historical (1950-2010)	N/A	530	N/A
MPI ESM LR (2010-2090)	2.6	1800	340%
	4.5	2700	510%
	8.5	9300	1750%
CSIRO MK3 (2010-2090)	2.6	2200	415%
	4.5	4100	770%
	8.5	9400	1800%
GFDL ESM2G (2010-2090)	2.6	2100	400%
	4.5	2000	380%
	8.5	6200	1200%

For Maricopa County, intra-urban variation in EHE frequency is significant. Variation in EHE frequency is measured by counting the number of EHE days in each parcel for the period of interest. For the historical time period, EHE days from 1950 to 2010 are counted for each parcel. For future scenarios, EHE days from 2010 to 2090 are counted for each parcel (using outputs from each model), then averaged across each projection scenario. Figures 4 and 5 show the number of EHE days for each parcel in Maricopa County under historical and future time periods, respectively. Figure 4 shows the number of EHE days for each parcel for the historical period (1950 to 2010). Figure 5 shows the number of EHE days for each parcel under the RCP 4.5 scenario (2010 to 2090), using the average of the three models. The color of each 1/8 degree by 1/8-degree parcel corresponds to the number of EHE days at that location for the period of interest. Thus, for the time period 1950-2010 (Figure 4), parcels with 45-81 EHE days across the entire period are indicated by the color blue, while parcels with 151-202 EHE days are indicated by the color red. For the historical period, EHE days range from about 45 to 200 days per parcel. The standard deviation between parcels is roughly 25 EHE days, with a coefficient of variation of 0.24. For the future period (2010 to 2090), total EHE days range from about 440 to 1100 days per parcel. Under future conditions, the coefficient of variation ranges between 0.08 (under the RCP 8.5 scenario) to 0.17 (under the RCP 2.6 scenario). Geospatial variation becomes less significant under future scenarios because more parcels experience extreme heat events for longer periods of time. Thus, although temperature may vary between parcels, this variation is not accounted for because EHEs are determined only by the threshold temperatures T1 and T2 (which are more easily exceeded under future scenarios). It is important to note that estimates of EHEs are constructed using only BCCA downscaled GCM output. In other words, geospatial variation in EHE days does not account for urbanization or urban land cover effects.

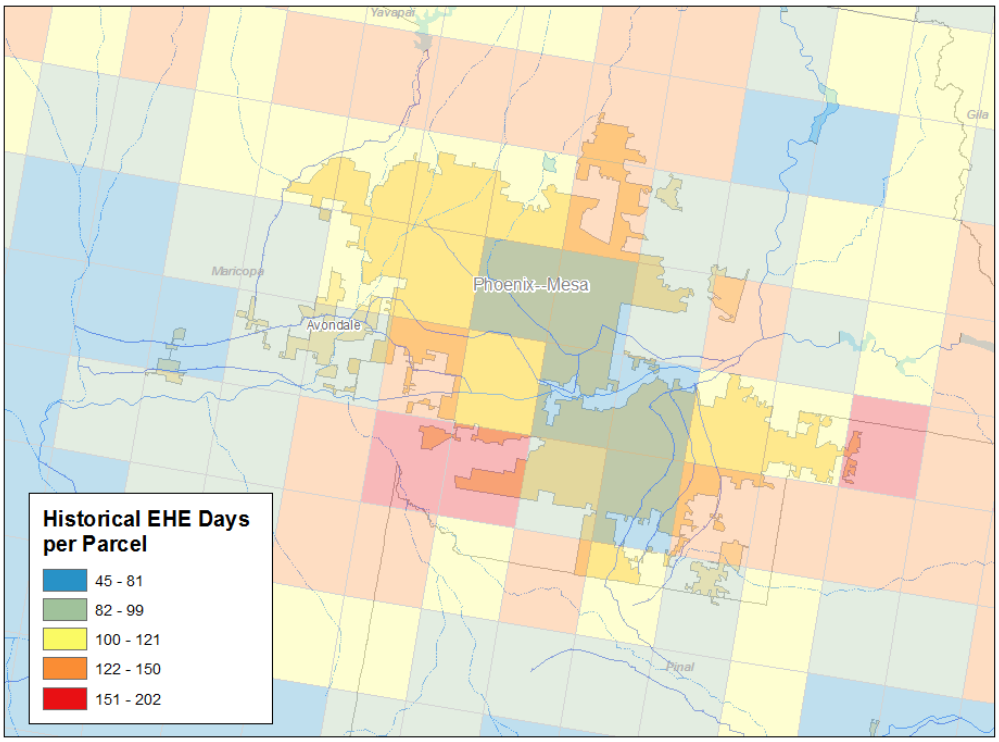

Figure 4. Historical Distribution of EHE Days for Maricopa County. Parcel colors indicate the total number of EHEs for the historical period 1950-2010.

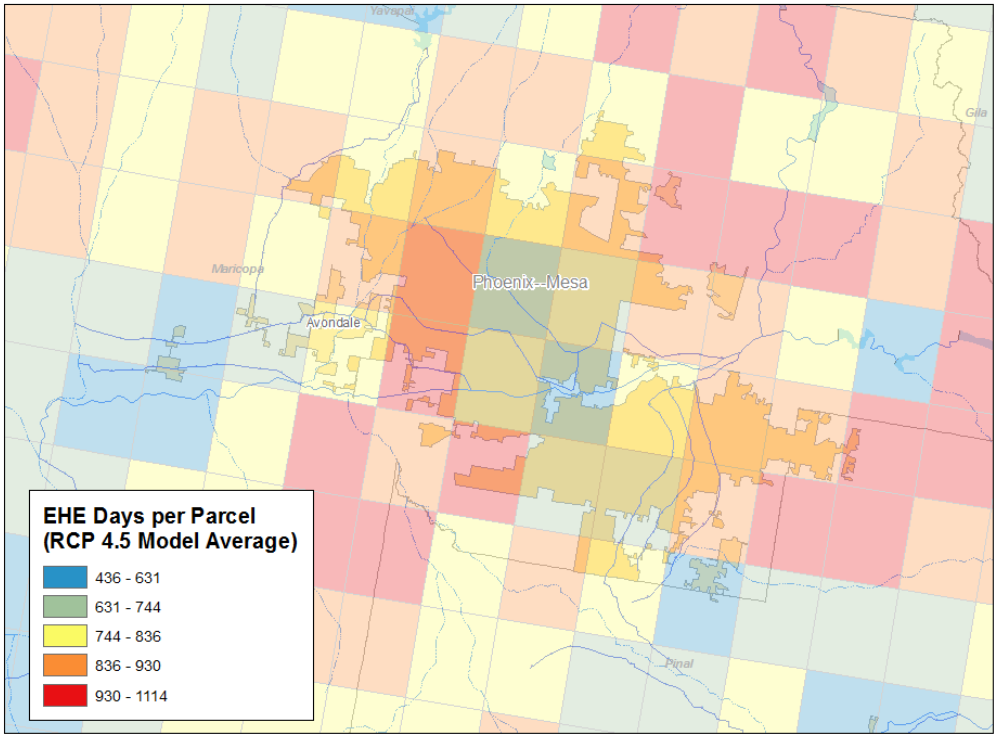

Figure 5. Future Distribution of EHE Days for Maricopa County, using the average number of EHEs encountered under the RCP 4.5 Scenario. Parcel colors indicate the total number of EHEs for the period 2010-2090.

3.1.2 Extreme Heat Events in Los Angeles County

For Los Angeles County, EHEs increase by 150-840% under future scenarios. As with Maricopa County, the frequency of EHEs increases with increasing atmospheric carbon concentrations. Compared to Maricopa County, less consistency is observed between GCM models. The coefficient of variation between models ranges between a low of 0.18 under the RCP 8.5 scenario to a high of 0.40 under the RCP 4.5 scenario (see Table 3). Figures 6 through 8 show the frequency of EHEs for Los Angeles County under both historical and projected time periods. As with Maricopa County, future EHEs are derived from GCM-modeled temperatures, and yearly EHEs are measured in terms of parcel-days. In Los Angeles County, there are 208 parcels and 365 potential EHE days (making the theoretical maximum number of EHEs 75,920 parcel-days per year). By the 2080s, EHE counts of 14,000-20,000 parcel days per year are encountered, meaning that by the end of the twenty-first century, 18-25% of the entire year can be considered an "extreme heat event" for most parcels in Los Angeles County.

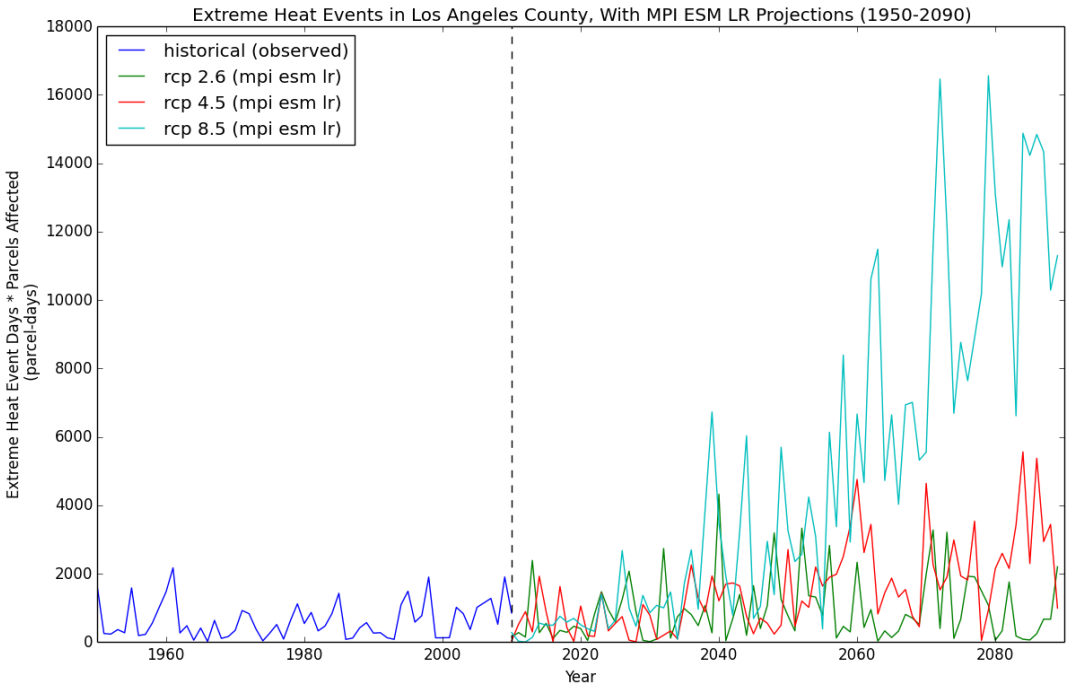

Figure 6. Extreme Heat Events in Los Angeles County, with MPI ESM LR Projections (1950-2090)

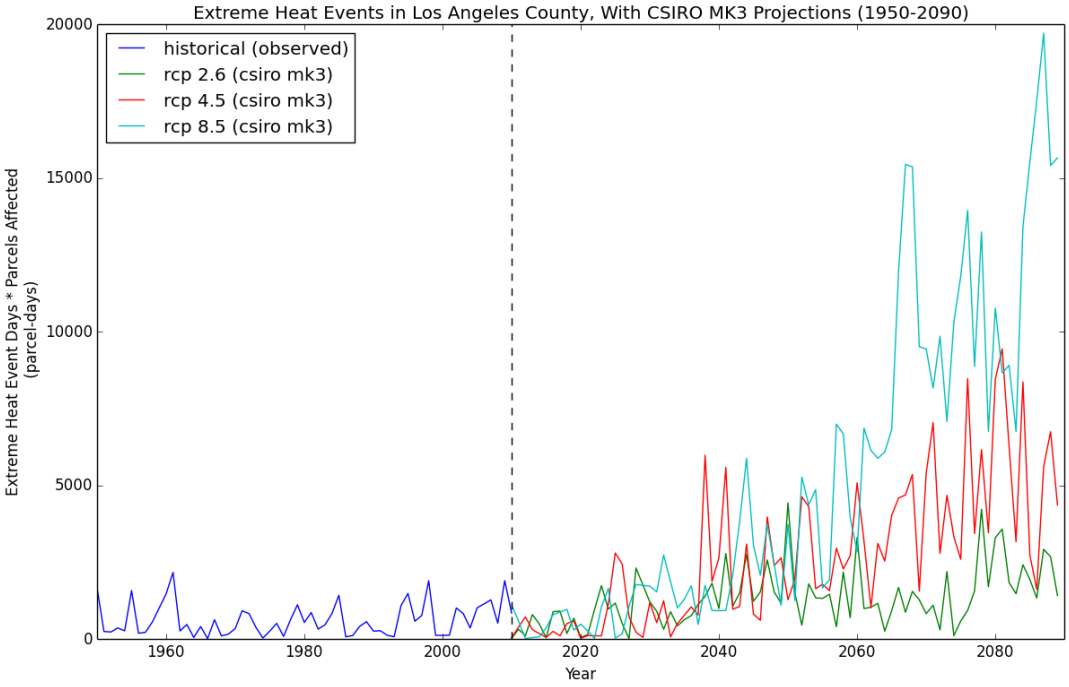

Figure 7. Extreme Heat Events in Los Angeles County, with CSIRO MK3 Projections (1950-2090)

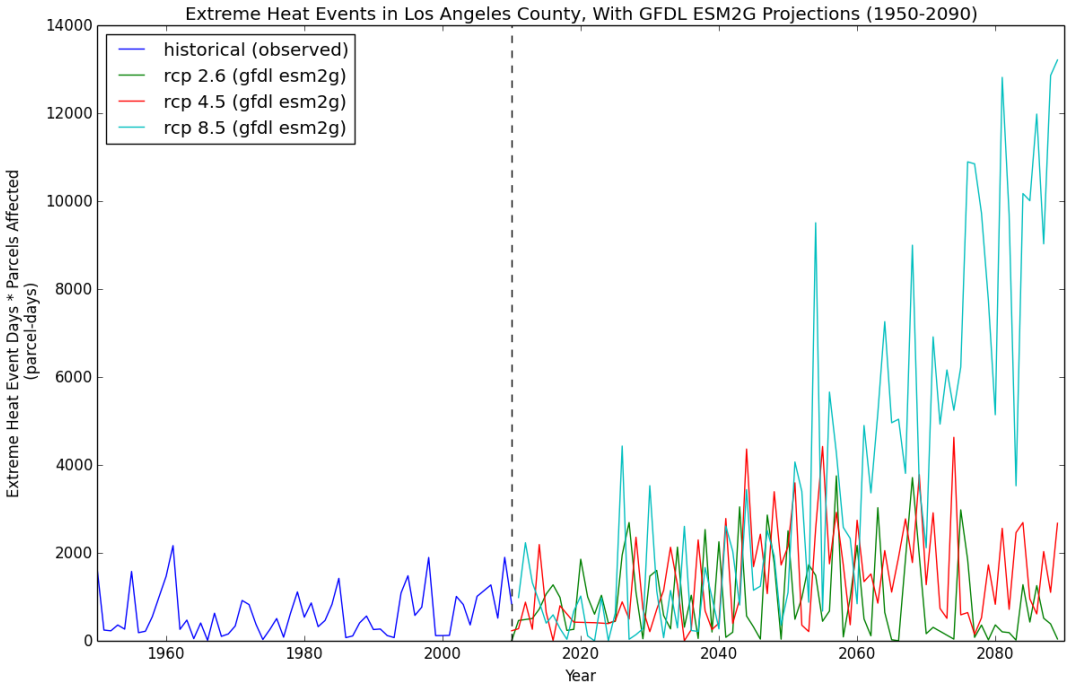

Figure 8. Extreme Heat Events in Los Angeles County, with GFDL ESM2G Projections (1950-2090).

Table 3. Breakdown of Extreme Heat Events by Model and Scenario for Los Angeles County.

Model/Scenario	RCP Scenario	Average Extreme Heat Events per Year (Parcel-Days)	Percent Increase in Extreme Heat Events
Historical (1950-2010)	N/A	630	N/A
MPI ESM LR (2010-2090)	2.6	940	150%
	4.5	1500	240%
	8.5	4900	780%
CSIRO MK3 (2010-2090)	2.6	1300	210%
	4.5	2800	440%
	8.5	5300	840%
GFDL ESM2G (2010-2090)	2.6	960	150%
	4.5	1450	230%
	8.5	3700	590%

Los Angeles County exhibits even greater spatial variability in EHE frequency than does Maricopa County. As with Maricopa County, variations in EHE frequency are measured by counting the number of EHE days in each parcel for the period of interest. Figures 9 and 10 show the number of EHE days for each parcel in Los Angeles County under historical and future time periods, respectively. Figure 9 shows the number of EHE days for each parcel in Los Angeles County for the historical period (1950 to 2010), while Figure 5 shows the number of EHE days for each parcel in Los Angeles County under the RCP 4.5 scenario (2010-2090), using the average of the three GCM models. For the historical period, total EHE days range from about 50 to 740 days per parcel. The standard deviation between parcels is roughly 100 EHE days, with a coefficient of variation of 0.51—roughly twice that of Maricopa County. The high degree of variation in EHE frequency is likely explained by the proximity of the ocean, which "smooths" the annual temperature distribution for coastal areas. For the future period (2010 to 2090), total EHE days range from about 110 to 1400 days per parcel. For this period, the coefficient of variation between parcels ranges between 0.30 (under the RCP 8.5 scenario) to 0.60 (under the RCP 2.6 scenario). For Los Angeles County, geospatial variation in EHEs is not as strongly affected by climate change. This could possibly be caused by the temperature-moderating effect of the ocean—parcels closer to the water will be less affected by extreme heat because the ocean serves as a "heat sink". It is worth noting that the spatial distribution of EHEs changes under the projected scenario. Whereas EHEs are more concentrated near the coast during the historical period, the future period shows a redistribution of EHEs toward the inland areas. When historical EHEs are examined in detail, it is found that many coastal EHEs occur during the spring and fall months. For coastal areas, the annual temperature distribution is much "smoother" than for inland areas—in other words, the difference in

temperature between summer and winter months is much smaller. Thus, for coastal areas, the threshold temperatures (T1 and T2) are small compared to the average annual temperature, making them more sensitive to advection of heat from other regions. Weather patterns that transfer warm air to coastal regions can cause EHEs to occur even during October or November. It is possible that GCM models cannot currently replicate weather patterns that bring unseasonably hot weather to coastal areas during Fall or Spring months. Thus, under future scenarios, EHEs are redistributed towards inland areas, where the weather is less moderate. Another possibility is that the downscaled GCM projections are accurate, and that the spatial distribution of EHEs will actually shift inland. Again, this could be caused by the temperature-moderating influence of the ocean—increases to air temperature will be smaller in coastal regions where the ocean acts as a "heat sink".

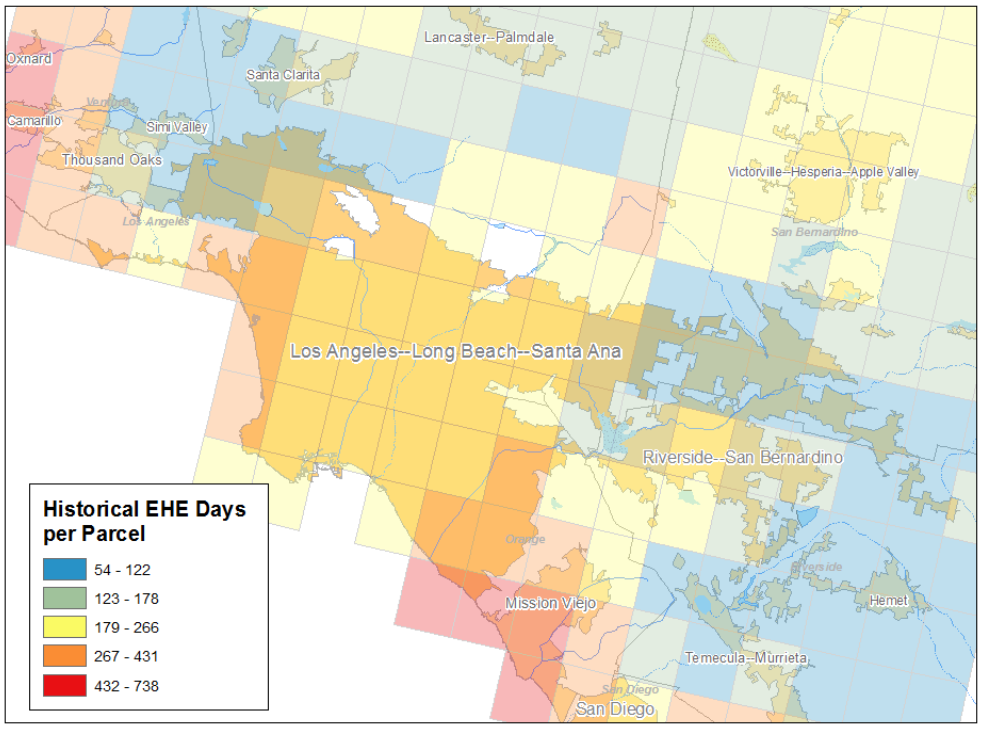

Figure 9. Historical Distribution of EHE Days for Los Angeles County. Parcel colors indicate the total number of EHEs for the historical period 1950-2010.

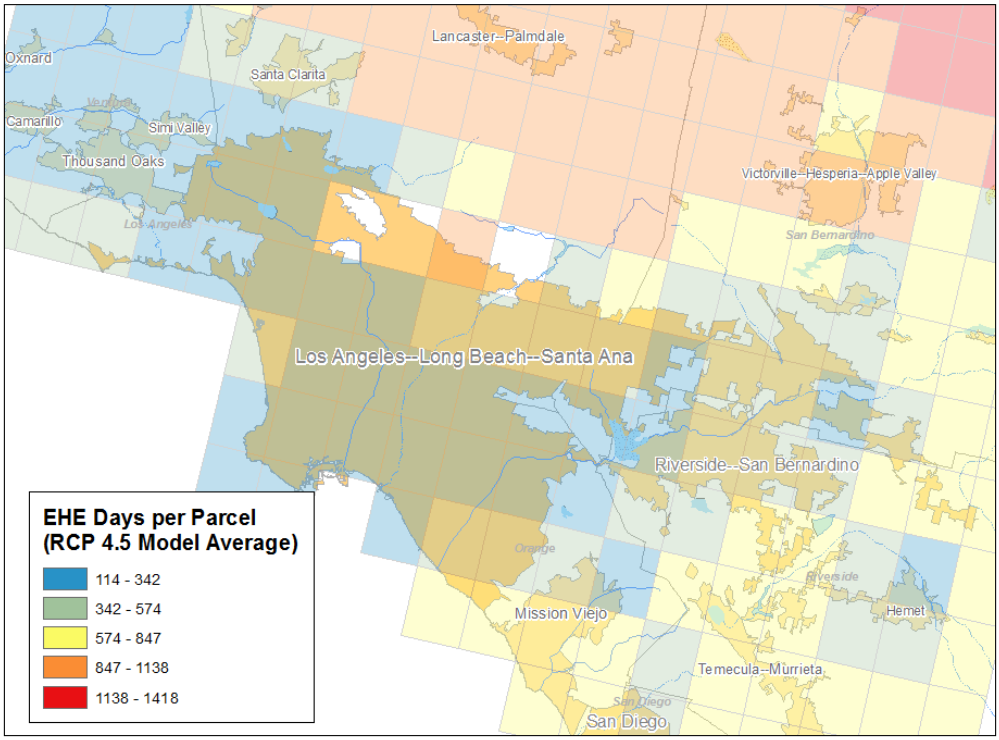

Figure 10. Future Distribution of EHE Days for Los Angeles County, using the average number of EHEs encountered under the RCP 4.5 Scenario. Parcel colors indicate the total number of EHEs for the period 2010-2090.

Table 4. Variation in Extreme Heat Days between models for each RCP Scenario.

City	RCP Scenario	Coefficient of Variation Between Models
Phoenix	2.6	0.10
	4.5	0.36
	8.5	0.22
Los Angeles	2.6	0.19
	4.5	0.40
	8.5	0.18

3.2 Conclusion

Both Phoenix and Los Angeles are expected to experience a marked increase in extreme heat events over the next century. EHE frequency is primarily affected by the concentration of atmospheric greenhouse gases, with EHEs increasing by up to 1800% under the RCP 8.5 scenario. However, large increases in EHEs (150-400%) are observed even under the most optimistic representative concentration pathway (RCP 2.6). Although this study highlights the importance of curbing GHG emissions, it also shows that infrastructure "readiness" must be achieved to help mitigate increases to EHEs that may ultimately be unavoidable. With more frequent EHEs on the horizon, identifying "at-risk" neighborhoods and investing in heat-resilient infrastructure may ultimately prove more effective than reducing GHG emissions. This study also highlights the need to account for intra-urban variation in meteorological characteristics. Even when land cover is not accounted for, spatial variation EHEs is significant. For Maricopa County, the historical number of EHEs per parcel varies from 45 days to 202 days (for the period 1950 to 2010). This means that some parcels experience nearly 4.5 times more EHEs than others, even when urbanization effects are not included. Los Angeles exhibits even greater geospatial variation in the frequency of EHEs, with a maximum/minimum ratio of 15 to 1 across all parcels. In Los Angeles, downscaled temperature projections seem to indicate a shift in EHEs away from the coast, and toward the inland areas. This spatial shift in EHEs could entrench existing environmental inequity issues, shifting even more burden onto lower-income residents living in the inland neighborhoods of Los Angeles. The results of this study highlight the need to take spatial and temporal variability in EHEs into account in assessments of heat vulnerability.

3.3 References

Braga, A. L. F., Zanobetti, A., Schwartz, J., et al. 2002. The effect of weather on respiratory and cardiovascular deaths in 12 US cities. Environmental Health Perspectives, 110, 859–863.

Brekke, L.D., Kiang, J.E., Olsen, J.R., Pulwarty, R.S., Raff, D.A., Turnipseed, D.P., Webb, R.S., and White, K.D., 2009, Climate change and water resources management—A federal perspective: U.S. Geological Survey Circular 1331, 65 p. (Also available online at http://pubs.usgs.gov/circ/1331/.)

California Climate Change Center (CCCC). 2009. Using Future Climate Projections to Support Water Resources Decision Making in California. CEC-500-2009-052-F.

CDC. 2013. Climate Change and Extreme Heat Events Guidebook. http://www.cdc.gov/climateandhealth/pubs/ClimateChangeandExtremeHeatEvents.pdf

Chuang, W.C., Gober, P., Chow, W.T.L., Golden, J. Sensitivity to heat: A comparative study of Phoenix, Arizona and Chicago, Illinois (2003-2006), (2013), doi: 10.1016/j.uclim.2013.07.003

Clarke, S.G., Zehnder, J.A. et al. 2010. Contribution of Land Use Changes to Near-Surface Air Temperatures During Recent Summer Extreme Heat Events in the Phoenix Metropolitan Area. Journal of Applied Meteorology and Climatology. 49, 1649-1664.

Covey, C., AchutaRao, K.M., Cubasch, U., Jones, P., Lambert, S.J., Mann, M.E., Phillips, T.J., Taylor, K.E. 2003. An Overview of Results from the Coupled Model Intercomparison Project (CMIP). Global and Planetary Change. 37, 103-133.

Curriero, F. C., Heiner, K. S., Samet, J. M., Zeger, S. L., Strug, L., Patz, J. A., et al. 2002. Temperature and mortality in 11 Cities of the eastern United States. American Journal of Epidemiology, 155, 80–87.

Duneier, Mitchell (2004). "Scrutinizing the Heat: On Ethnic Myths and the Importance of Shoe Leather". Contemporary Sociology (American Sociological Association) 33 (2): 139–150. doi: 10.1177/009430610403300203. JSTOR 3593666

Greene, S., Kalkstein, L.S., Mills, D.M., Samenow, J. 2011. An Examination of Climate Change on Extreme Heat Events and Climate-Mortality Relationships in Large U.S. Cities. Weather, Climate and Society. 3, 281-292. DOI: 10.1175/WCAS-D-11-00055.1

Hajat S., Sheridan S.C., Allen, M.J., Pascal, M., Laaidi, K., Yagouti, A., Bickis, U., Tobias, A., Bourque D., Armstrong B.G., Kosatsky T. 2010. American Journal of Public Health: Research and Practice. 100, 6, 1137-1144.

Harlan, S. L., Brazel, A. J., Prashad, L., Stefanov, W. L., Larsen, L., et al. 2006. Neighborhood microclimates and vulnerability to heat stress. Social Science & Medicine, 63, 2847–2863.

Harlan, S. L., Budruk, M., Gustafson, A., Larson, K., Ruddell, D., Smith, V. K., Yabiku, S. T., Wutich, A., et al. 2007. Phoenix Area Social Survey 2006 Highlights: Community and Environment in a Desert Metropolis. Central Arizona – Phoenix Long-Term Ecological Research Project, Contribution No. 4. Global Institute of Sustainability, Arizona State University.

Heynen, N. C. & Lindsey, G. 2003. Correlates of Urban Forest Canopy Cover: Implications for Local Public Works. Public Works Management & Policy, 8, 33-47.

Hondula, D.M. and Davis, R.E. 2010. Climatology of winter transition days for the contiguous USA, 1951-2007. Theor Appl Climatol. doi: 10.1007/s00704-010-0278-7

Jenerette, G. D., Harlan, S. L., Brazel, A. J., Jones, N., Larsen, L., Stefanov, W. L., et al. 2007. Regional relationships between vegetation, surface temperature, and human settlement in a rapidly urbanizing ecosystem. Landscape Ecology, 22, 353–365.

Klinenberg, Eric (2002). Heat Wave: A Social Autopsy of Disaster in Chicago. Chicago, IL: Chicago University Press. ISBN 0-226-44322-1.

Kovats, R. S. & Hajat, S. 2008. Heat Stress and Public Health: A Critical Review. Annual Review of Public Health, 29, 41-55.

Larson, J. 2006. Setting the record straight: more than 52,000 Europeans died from heat in summer 2003. Earth Policy Institute. Available at: http://www.earth-policy.org/Updates/2006/Update56.htm.

Liang, X., D. P. Lettenmaier, E. F. Wood, and S. J. Burges, 1994: A Simple hydrologically Based Model of Land Surface Water and Energy Fluxes for GSMs, *J. Geophys. Res.*, **99**(D7), 14,415-14,428.

Meehl, G. A., and Tebaldi, C. 2004. More intense, more frequent, and longer lasting heat waves in the 21st century. Science, 305, 994–997.

Maurer, E.P., A.W. Wood, J.C. Adam, D.P. Lettenmaier, and B. Nijssen, 2002, A Long-Term Hydrologically-Based Data Set of Land Surface Fluxes and States for the Conterminous United States, *J. Climate* 15, 3237-3251.

Michelozzi, P., DeSario, M., Accetta, G., De'Donato, F., Kirchmayer, U., D'Ovidio, M., Perucci,C., et al. 2006. Temperature and summer mortality: geographical and temporal variations in four Italian cities. Journal of Epidemiology and Community Health, 60, 417–423

NWS, cited 2009: Weather fatalities. [Available online at http://www.nws.noaa.gov/om/hazstats.shtml.]

Pincetl, S. 2010b. Implementing municipal tree planting: Los Angeles million-tree initiative. Environmental management, 45, 227-238.

Pincetl, S., Gillespie, T., Pataki, D., Saatchi, S. & Saphores, J.-D. 2012. Urban tree planting programs, function or fashion? Los Angeles and urban tree planting campaigns. GeoJournal, 1-19.

Reclamation, 2013. 'Downscaled CMIP3 and CMIP5 Climate and Hydrology Projections: Release of Downscaled CMIP5 Climate Projections, Comparison with preceding Information, and Summary of User Needs', prepared by the U.S. Department of the Interior, Bureau of Reclamation, Technical Services Center, Denver, Colorado. 47pp.

Semenza, J.C., Rubin, C.H., Falter, K.H., Selanikio, J.D., Flanders, W.D., How,H.L., Wilhelm, J. L., et al. 1996. Heat-related deaths during the July 1995 heat wave in Chicago. American Journal of Preventive Medicine, 16(4), 269–277.

Semenza, J. C., McCullough, J. E., Flanders, W. D., McGeehin, M., Lumpkin, J. R. et al. 1999. Excess hospital admissions during the July 1995 heat wave in Chicago. American Journal of Preventive Medicine, 16(4), 269–277.

Sheridan, S. C. and Kalkstein, L. S. 2004. Progress in heat watch-warning system technology. Bulletin of the American Meteorological Society, 85, 1931–1941.

Smoyer-Tomic, K. E., and Rainham, D. G. C. 2001. Beating the heat: Development and evaluation of a Canadian hot weather health-response plan.Environmental Health Perspectives, 109, 1241–1248.

Smoyer, K. E., Rainham, D. G., Hewko, J. N., et al. 2000. Heat-related stress mortality in five cities in southern Ontario: 1980–1996.Institutional Journal of Meteorology, 44(1809), 190–197.

Spatial Synoptic Classification (SSC) Homepage. 2013. http://sheridan.geog.kent.edu/ssc.html

U.S. EPA. 2006. Excessive Heat Events Guidebook. EPA 430-B-06-005. U.S. Environmental Protection Agency, Washington, DC.

Whitman, S., G. Good, E. R. Donoghue, N. Benbow, W. Shou, and S. Mou, 1997: Mortality in Chicago attributed to the July 1995 heat wave. Amer. J. Public Health, 87, 1515–1518.

4 Appendix A

Script Used to Calculate T1 and T2 for Phoenix and Los Angeles:

```
#1. Store phx/la entries for particular historical year in HDF5 file.

import numpy as np
import pandas as pd
import netCDF4
from datetime import date
import os

la_latlon = #List of latitude/longitude tuples comprising Los Angeles
phx_latlon = #List of latitude/longitude tuples comprising Phoenix


def clip_region(regname, regloc):

        region_h5 = pd.HDFStore('%s.h5' % (regname))

        for fn in os.listdir('.'):
                if fn.endswith('nc'):
                        region_df = pd.DataFrame()
                        f_max = netCDF4.Dataset(fn, 'r')
                        pan = pd.Panel(f_max.variables['tasmax'][:],
items=f_max.variables['time'], major_axis=f_max.variables['latitude'][:],
minor_axis=f_max.variables['longitude'][:])
                        df = pan.to_frame()
                        df_stack = df.stack()
                        df_flat=df_stack.reset_index()
                        df_flat.columns=['latitude', 'longitude', 'time', 'tmax']

                        for i in regloc:
                                region_df = region_df.append(df_flat.ix[(df_flat['latitude']==i[0])
& (df_flat['longitude']==i[1])])

                        region_h5['%s_%s' % (regname, fn[-7:-3])] = region_df


clip_region('la', 'la_latlon')
clip_region('phx', 'phx_latlon')


#2. Reload HDF5 stores

la = pd.HDFStore('la.h5')
phx = pd.HDFStore('phx.h5')


#3. Combine period of record into a single dataframe.

la_all = pd.concat([la[i] for i in la.keys()], axis=0, ignore_index=True)
la['la_all'] = la_all

phx_all = pd.concat([phx[i] for i in phx.keys()], axis=0, ignore_index=True)
phx['phx_all'] = phx_all


la_record = pd.DataFrame()
phx_record = pd.DataFrame()

record = range(1960, 1991)

for i in record:
        la_year = 'la_' + '%s' % (i)
        la_record = la_record.append(la[la_year])

la_record = la_record.reset_index()
```

```
for i in record:
        phx_year = 'phx_' + '%s' % (i)
        phx_record = phx_record.append(phx[phx_year])

phx_record = phx_record.reset_index()

#4. Convert time to datetime.

la_record['date'] = [date.fromordinal(int(708205 + i)) for i in la_record.time]
phx_record['date'] = [date.fromordinal(int(708205 + i)) for i in phx_record.time]

#5. Convert longitude format.

la_record['longitude'] = la_record['longitude'] + 360
phx_record['longitude'] = phx_record['longitude'] + 360

#6. Select summer months (June through August).

la_summer_idx = []
phx_summer_idx = []

for i, row in la_record.iterrows():
        if 6 <= row['date'].month <= 8:
                la_summer_idx.append(i)

for i, row in phx_record.iterrows():
        if 6 <= row['date'].month <= 8:
                phx_summer_idx.append(i)

la_summer = la_record.ix[la_summer_idx]
phx_summer = phx_record.ix[phx_summer_idx]

#7. Calculate 97.5th and 81st historical percentiles.

la_T1 = la_summer.groupby(['latitude', 'longitude']).quantile(0.975)
la_T2 = la_summer.groupby(['latitude', 'longitude']).quantile(0.81)

del la_T1['index']
del la_T1['time']
del la_T1['latitude']
del la_T1['longitude']
la_T1 = la_T1.reset_index()

del la_T2['index']
del la_T2['time']
del la_T2['latitude']
del la_T2['longitude']
la_T2 = la_T2.reset_index()

phx_T1 = phx_summer.groupby(['latitude', 'longitude']).quantile(0.975)
phx_T2 = phx_summer.groupby(['latitude', 'longitude']).quantile(0.81)

del phx_T1['index']
del phx_T1['time']
del phx_T1['latitude']
del phx_T1['longitude']
phx_T1 = phx_T1.reset_index()

del phx_T2['index']
del phx_T2['time']
del phx_T2['latitude']
del phx_T2['longitude']
phx_T2 = phx_T2.reset_index()

#8. Store percentiles

la_T1.to_csv('la_T1.csv')
la_T2.to_csv('la_T2.csv')
```

```
phx_T1.to_csv('phx_T1.csv')
phx_T2.to_csv('phx_T2.csv')
```

5 Appendix B

Script Used to Query Historical/Projected Data for Extreme Heat Events (Historical Query Shown Below):

```
import numpy as np
import pandas as pd
import netCDF4
from datetime import date
import os

la_T1 = pd.read_csv('la_T1.csv')
la_T2 = pd.read_csv('la_T2.csv')
phx_T1 = pd.read_csv('phx_T1.csv')
phx_T2 = pd.read_csv('phx_T2.csv')

la_T1['latlon'] = la_T1[['latitude', 'longitude']].apply(tuple, axis=1)
la_T2['latlon'] = la_T2[['latitude', 'longitude']].apply(tuple, axis=1)
del la_T1['latitude']
del la_T1['longitude']
del la_T1['Unnamed: 0']
del la_T2['latitude']
del la_T2['longitude']
del la_T2['Unnamed: 0']
la_T1['t1'] = la_T1['tmax']
del la_T1['tmax']
la_T2['t2'] = la_T2['tmax']
del la_T2['tmax']

phx_T1['latlon'] = phx_T1[['latitude', 'longitude']].apply(tuple, axis=1)
phx_T2['latlon'] = phx_T2[['latitude', 'longitude']].apply(tuple, axis=1)
del phx_T1['latitude']
del phx_T1['longitude']
del phx_T1['Unnamed: 0']
del phx_T2['latitude']
del phx_T2['longitude']
del phx_T2['Unnamed: 0']
phx_T1['t1'] = phx_T1['tmax']
del phx_T1['tmax']
phx_T2['t2'] = phx_T2['tmax']
del phx_T2['tmax']

#9. Prepare projections

la = pd.HDFStore('la.h5')

la_all = la['la_all']

la_all['date'] = [date.fromordinal(int(708205 + i)) for i in la_all.time]
la_all['longitude'] = la_all['longitude'] + 360
la_all['latlon'] = zip(la_all['latitude'], la_all['longitude'])

la_all = pd.merge(la_all, la_T1, on='latlon')
la_all = pd.merge(la_all, la_T2, on='latlon')



phx = pd.HDFStore('phx.h5')

phx_all = phx['phx_all']

phx_all['date'] = [date.fromordinal(int(708205 + i)) for i in phx_all.time]
```

```
phx_all['longitude'] = phx_all['longitude'] + 360
phx_all['latlon'] = zip(phx_all['latitude'], phx_all['longitude'])

phx_all = pd.merge(phx_all, phx_T1, on='latlon')
phx_all = pd.merge(phx_all, phx_T2, on='latlon')


#10. Query projections for extreme heat events

crit = []

def sel(rcp):
        for i in range(len(rcp.index)):
                if rcp['tmax'].ix[i] > rcp['t1'].ix[i]:
                        if rcp['tmax'].ix[i+1] > rcp['t1'].ix[i+1]:
                                if rcp['tmax'].ix[i+2] > rcp['t1'].ix[i+2]:
                                        crit.extend([rcp.index[i]])
                                        cumsum = 0.0
                                        ct = 0
                                        for index, rows in rcp[i:].iterrows():

                                                cumsum += rows['tmax']
                                                ct = ct + 1
                                                mov_avg = cumsum/float(ct)
                                                if mov_avg > rcp['t1'].ix[i]:
                                                        if rows['tmax'] > rows['t2']:
                                                                if ct>1:
                                                                        crit.extend([index])
                                                                        #print ct
                                                                        continue
                                                                else:
                                                                        continue
                                                        else:
                                                                i = index
                                                                break
                                                else:
                                                        i = index
                                                        break
                                else:
                                        continue
                        else:
                                continue
                else:
                        continue


sel(la_all)

EHE_la_hist = la_all.ix[sorted(set(crit))]
EHE_la_hist.to_csv('EHE_la_hist.csv')

crit = []
del EHE_la_hist

la.close()


EHE_phx_hist = phx_all.ix[sorted(set(crit))]
EHE_phx_hist.to_csv('EHE_phx_hist.csv')

crit = []
del EHE_phx_hist

phx.close()
```